THE JOURNAL OF COMPARATIVE NEUROLOGY 284:504–518 (1989)

Development of GABA Immunoreactivity in Brainstem Auditory Nuclei of the Chick: Ontogeny of Gradients in Terminal Staining

REBECCA A. CODE, GAIL D. BURD, AND EDWIN W RUBEL
Hearing Development Laboratories, University of Washington School of Medicine, Seattle, Washington 98195 (R.A.C., E.WR.); Departments of Anatomy and Molecular & Cell Biology, University of Arizona, Tucson, Arizona 85721 (G.D.B.)

ABSTRACT

The development of gamma-aminobutyric acid-immunoreactivity (GABA-I) in nucleus magnocellularis (NM) and nucleus laminaris (NL) of the chick was studied by using an antiserum to GABA. In posthatch chicks, GABA-I is localized to small, round punctate structures in the neuropil and surrounding nerve cell bodies. Electron microscopic immunocytochemistry demonstrates that these puncta make synaptic contact with neuronal cell bodies in NM; thus, they are believed to be axon terminals. GABAergic terminals are distributed in a gradient of increasing density from the rostromedial to the caudolateral regions of NM.

The distribution of GABA-I was studied during embryonic development. At embryonic days (E) 9–11, there is little GABA-I staining in either NM or NL. Around E12–14, a few fibers are immunopositive but no gradient is seen. More GABA-I structures are present at E14–15. They are reminiscent of axons with varicosities along their length, preterminal axonal thickenings and fiber plexuses. At E15, terminals become apparent circumscribing neuronal somata and are also discernible in the neuropil of both nuclei. In E16–17 embryos, terminals are the predominantly labeled GABA-I structures and they are uniformly distributed throughout NM. The density of GABAergic terminals increases in caudolateral regions of NM such that by E17–19, there is a gradient of increasing density of GABA-I terminals from the rostromedial to caudolateral regions of NM. The steepness of this gradient increases during development and is the greatest in posthatch (P) chicks.

Cell bodies labeled with the GABA antiserum are located around the borders of both NM and NL and in the neuropil between these two nuclei. Occasionally, GABA-I neurons can be found within these auditory brainstem nuclei in both embryonic and posthatch chicks. Nucleus angularis (NA) contains some GABAergic cells.

The appearance of GABA-I terminals around E15 is correlated in time with the formation of end-bulbs of Held on NM neurons. Thus, the ontogeny of presumed inhibitory inputs to chick auditory brainstem nuclei temporally correlates with, and could modulate the development of, excitatory auditory afferent structure and function.

Key words: nucleus magnocellularis, nucleus laminaris, GABAergic terminals, inhibitory afferents, immunocytochemistry

Inhibitory synaptic connections play an important role in information processing at many levels of the auditory system. In the cochlear nucleus, physiological (Pfeiffer, '66), morphological (Cant, '81; Parks, '81; Wenthold et al., '86), and pharmacological (Wenthold and Martin, '84) studies

Accepted January 20, 1989.

Address reprint requests to Edwin W Rubel, Hearing Development Laboratories, RL-30, University of Washington School of Medicine, Seattle, WA 98195.

A preliminary report of these findings has appeared (Code et al., '87).

indicate that inhibitory synapses are present. It appears that some of the inhibition within the cochlear nucleus of the cat (Godfrey et al., '77), rat (Godfrey et al., '78), and guinea pig (Fisher and Davies, '76) is mediated by gamma-aminobutyric acid (GABA), a major inhibitory neurotransmitter in the central nervous system. GABA satisfies several of the criteria for considering it a neurotransmitter in the cochlear nucleus, including in vitro studies demonstrating a calcium-dependent release of endogenous GABA (Wenthold, '79; Canzek and Reubi, '80).

Immunocytochemical techniques have been used to elucidate the location of GABAergic terminals in the auditory system. For example, glutamic acid decarboxylase (GAD), the synthetic enzyme for GABA, has been studied in the cochlear nuclei of the cat (Adams and Mugnaini, '87), rat (Mugnaini, '85; Moore and Moore, '87), and gerbil (Roberts and Ribak, '87). Only recently has the specific immunocytochemical localization of GABA itself been described. In the cochlear nuclei of the guinea pig (Thompson et al., '85; Peyret et al., '86; Wenthold et al., '86) and chicken (Müller, '87), nerve cell bodies were surrounded by densely immunostained punctate structures, presumed to be GABAergic terminals. While the presence of GABA immunoreactivity has been documented in mature animals, little is known about the initial formation or developmental patterns of GABA-immunoreactive (GABA-I) terminals in embryonic auditory brainstem nuclei.

The chick is a useful animal in which to study the development of GABAergic innervation in auditory brainstem nuclei because the major afferents to nucleus magnocellularis (NM) and nucleus laminaris (NL) have been well characterized both physiologically (Rubel and Parks, '75; Hackett et al., '82) and anatomically (Ramón y Cajal, '08; Boord and Rasmussen, '63; Parks and Rubel, '78; Parks, '81; Jhaveri and Morest, '82b). The only excitatory input to NM that has been identified is from ipsilateral eighth nerve fibers (Born and Rubel, '84; Born, '86). NM in turn provides bilateral excitatory input to NL (Parks and Rubel, '75; Hackett et al., '82; Young and Rubel, '83). The other major input to both nuclei is immunoreactive to GABA (Code et al., '87). Other afferents are rare or nonexistent (Parks, '81; Code and Rubel, '89). Thus, the synaptic connections of these two auditory brainstem nuclei are relatively simple. In addition, both NM and NL have a rather homogeneous population of cell types (Smith and Rubel, '79; Jhaveri and Morest, '82a). No major class of interneuron has been described in these nuclei.

The present study describes the development of GABA-I terminals and fibers in the avian NM and NL, presumed homologues of the mammalian anteroventral cochlear nucleus and medial superior olive, respectively. GABA-I is first discernible in fibers in these nuclei around embryonic day (E) 12. Around E15, GABAergic terminals appear whose distribution changes markedly during the development of NM. In posthatch chicks, GABA-I terminals have become organized into a gradient of increasing density in a rostromedial-to-caudolateral direction across NM.

MATERIALS AND METHODS

Immunocytochemistry

Development of GABA-I was studied in NM and NL in 21 chick embryos (H & N breed) from embryonic day 9 (E9) to E19 and in 20 posthatch chicks from hatching (P0) to over 1 year of age (Table 1). Embryonic ages were determined according to the Hamburger and Hamilton ('51) staging series by staging each embryo and then assigning it the median age which is reflected by this stage in their series.

TABLE 1. Age Distribution of Chicks

Age	N
E9–11	5
E12–15	6
E16	5
E17–19	5
P0–3	3
P7–10	8
P11–14	2
P16–19	3
P26	1
P45	2
Over 1 year old	1
Total	41

Embryos and posthatch chicks were anesthetized with an intramuscular injection of ketamine hydrochloride (Vetalar; 80 mg/kg body weight) and an intraperitoneal injection of sodium pentobarbital (Nembutal; 20 mg/kg body weight). The animals were perfused transcardially with buffered normal saline followed by a mixture of 1% paraformaldehyde and 1.25% glutaraldehyde in 0.1 M phosphate buffer (pH 7.3–7.4) at room temperature. The brains were removed from the skull, blocked, and placed in the same fixative at 4°C overnight.

Standard immunocytochemical procedures were followed according to the avidin-biotin-peroxidase complex (ABC) method (Hsu et al., '81) with reagents from Vectastain kits (Vector Labs). All incubations were performed at room temperature. A one-in-three series of vibratomed or frozen sections, 30 μm thick, through the medulla was rinsed four times (20 minutes each) in phosphate buffer and then incubated for 1 hour in a presoak solution consisting of 3% normal goat serum (NGS) made in 0.5 M Tris buffer (pH 7.6). The sections were then incubated for 13–21 hours in rabbit antiserum to GABA conjugated to bovine serum albumin (GABA-BSA) (Immunonuclear, Inc.), diluted 1:2,000–1:4,000 in the presoak solution. Following two 20-minute rinses in Tris buffer and two 20-minute rinses in phosphate buffer, the sections were incubated for 1 hour in secondary antiserum consisting of biotinylated goat antirabbit immunoglobulin G (IgG) diluted 1:200 in phosphate buffer. The sections were then rinsed four times in buffer over the course of 30 minutes and incubated for 1 hour in ABC, diluted as recommended by Vector Labs. After four rinses of buffer during a 30-minute period, the sections were reacted in a 0.02% di-aminobenzidine (DAB) solution to which was added hydrogen peroxide at a final concentration of 0.003%. Following reaction times of 10–20 minutes, the sections were rinsed in four 5-minute changes of buffer, mounted onto poly-L-lysine-coated slides, dried, and coverslipped with DPX (BDH Limited; Poole, England) or Permount.

In addition, sections from three animals (ages E13, E15, and E17) were incubated in a rabbit anti-GABA antiserum conjugated to keyhole limpet hemocyanin (GABA-KLH) or in a mouse anti-GAD-2 antiserum, a monoclonal antibody directed against chick glutamic acid decarboxylase (GAD) (Gottlieb et al., '86) (two animals; ages E18 and P4). Immunocytochemical procedures similar to those described above were used with the following exceptions: tissue to be pro-

cessed with the GAD-2 antiserum was fixed with 1% paraformaldehyde and postfixed in the same fixative for 4 hours at 4°C. It was then placed in cold phosphate buffer overnight. Sections were not incubated in a presoak solution but were put directly into the GAD-2 antiserum, which was diluted 1:2,000–1:4,000 in 0.3% Triton X-100 for approximately 20 hours at 4°C. Biotinylated horse antimouse IgG, diluted 1:200 in buffer, was used as the secondary antibody. The remaining procedure was as described above.

Control studies included 1) tissue incubated in 3% normal goat serum without the GABA antiserum; 2) tissue incubated in GABA antiserum preadsorbed with GABA-BSA, diluted 1:10, 1:100, or 1:1,000. These controls resulted in the absence of GABA-I staining (Fig. 2B), thus indicating that the antiserum used is highly specific for GABA.

In other controls, tissue was incubated in GABA antiserum preadsorbed with either glutamine, glutamate, taurine, or β-alanine. These controls resulted in staining that was similar to that in tissue incubated in GABA antiserum alone, indicating no cross-reactivity between the GABA antiserum and these structurally similar amino acids.

Electron microscopic immunocytochemistry

Tissue from two posthatch chicks (P2) was processed for electron microscopic immunocytochemistry (EM-ICC). After perfusion and postfixation as described above, 30 μm-thick Vibratomed sections were incubated in GABA antiserum for 41 hours, followed by the standard ICC procedures (see above). After reacting in DAB, the sections were rinsed three times in 0.1 M PB and then osmicated in 1% osmium for 1 hour at room temperature. After four rinses of PB, the sections were dehydrated in cold ethanols (50%, 70%, 80%, 95% for 5 minutes each, then two changes of 100%, 15 minutes each) and allowed to come to room temperature. Sections were placed in propylene oxide (PO) (two changes, 5 minutes each) and then into a mixture of PO and Epon (3:1) for 1 hour followed by a mixture of PO and Epon (1:3) overnight in a dessicator. The sections were flat-embedded between two Aclar plastic sheets in fresh Epon which was then polymerized at 60°C for 2 days. After polymerization, the sections were examined with a stereomicroscope and trimmed to include NM and a thin ring of tissue surrounding it. The tissue block was then glued onto the flat surface of a polymerized Epon capsule with cyanoacrylate glue. Thin sections were obtained with a Reichert Ultracut E microtome and were examined and photographed unstained with a JEOL 1200 electron microscope.

Quantitative analyses

GABA-I terminals. In the present study, we wished to quantify the density of GABAergic terminals in NM. GABAergic terminals were therefore strictly defined as small, round or oval structures with well-defined borders that abutted NM cell bodies or were in the neuropil and that were immunostained above background levels. If there was any doubt as to whether a stained structure was a terminal or an artifact, it was not counted.

GABA-I terminals were counted with the aid of a Zeiss Videoplan interactive morphometry system. By using a 100× objective (N.A. 1.3) and a videocamera attached to the microscope, an image of the tissue was displayed on a CRT screen. GABA-I terminals were then counted on both sides of the tissue section by using the following sampling method. Regions of NM from which GABA-I terminals were to be counted were predetermined prior to analysis so as to preclude any bias in tissue selection. Terminals were counted in three sampling areas from each of three mediolateral regions of NM at three posterior-anterior (P-A) levels of the nucleus.

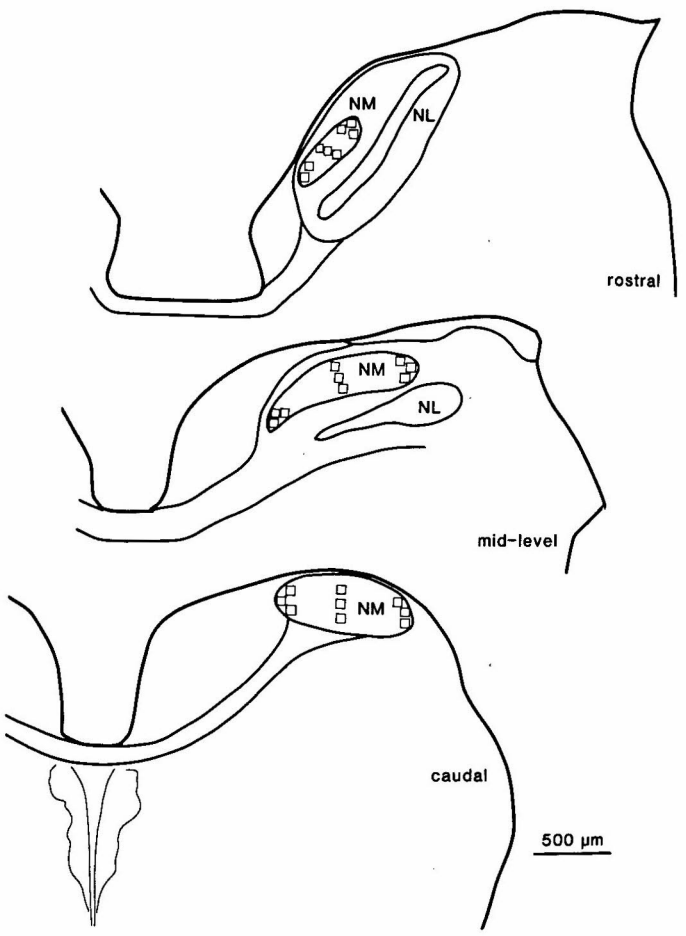

Fig. 1. Sampling areas within three caudorostral levels of nucleus magnocellularis (NM). The caudal level represents 20% of the total posterior-anterior (P-A) length of NM; the midlevel is 50%; the rostral level is 80%. Each square represents the approximate location of a 2,500 μm^2 sampling area from which GABA-I terminals were counted. Data from the three squares were averaged in each of the nine zones depicted here to obtain the density of GABA-I terminals. These data are illustrated in Figure 7.

The posterior-anterior (P-A) levels of NM were determined by the extreme caudal and rostral poles of the nucleus viewed in adjacent Nissl-stained sections (Fig. 1). These levels are expressed as a percentile of the total posterior-anterior length (% P-A) of the nucleus in order to allow interanimal comparisons at similar P-A levels. The caudal level was at 20% of the total P-A length; the midlevel was at 50%; the rostral level was at 80%. Sections from any given animal were selected as close to these three % P-A levels as possible. If sections were not available at these P-A levels due to tearing during sectioning or loss during immunocytochemical processing, the next closest section was selected for quantitative analysis. The % P-A level of any section selected for analysis did not vary by more than 7% from the three predetermined P-A levels. Within each P-A level, three zones of the nucleus were chosen from which to count

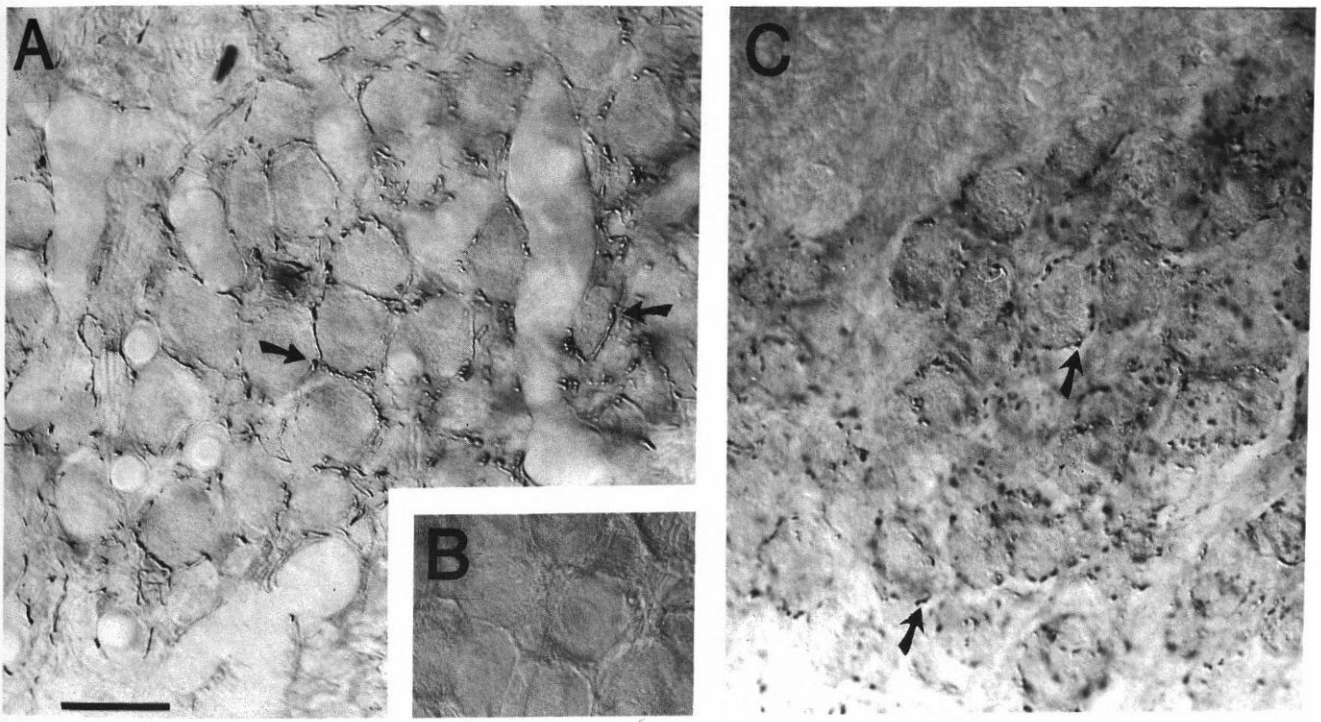

Fig. 2. **A:** Immunostaining in NM of an E17.5 chick obtained by using an antiserum to GABA-KLH diluted 1:1,000. Most GABA-I terminals (arrows) surround cell bodies. Scale bar (applies to A–C) = 10 μm. **B:** Virtual lack of immunostaining in NM of an E17.5 chick due to preadsorption of the GABA antiserum with GABA-BSA, diluted 1:1,000. Adjacent section to that shown in panel A. **C:** Immunoreactive terminals (arrows) circumscribing NM neurons in an E18 chick obtained by using a monoclonal antibody to GAD-2 diluted 1:2,000. NM cells appear smaller than those in panel A due to tissue shrinkage from frozen sectioning.

GABA-I terminals: medial, central, and lateral. As exemplified in Figure 1, the medial and lateral zones were the most medial and most lateral zones of the nucleus in that section, respectively. The central zone was defined to be halfway between the medial and lateral borders of the nucleus in that section.

In each of these three zones within a selected section (nine zones/NM nucleus), GABAergic terminals were counted and averaged in three separate areas, each 2,500 μm^2 (a square, 50 μm on a side). Within the central zone, the three sampling areas were on a line roughly perpendicular to a line connecting the medial and lateral borders of NM in that section (see Fig. 1). The selection of these areas was strictly adhered to except in the situation when a sampling area was over a large blood vessel. In that case, the sampling area would be moved until it was no longer over the blood vessel but still within the appropriate mediolateral zone of NM as defined above.

For each animal, counts from the three sampling areas were averaged, providing a single value for each of nine different zones of NM. Due to the size limitations of the rostromedial zone, GABA-I terminals were counted and averaged from only two sampling areas (see Fig. 1). The values are expressed as the average number of terminals per sample area, i.e., density. Quantitative analyses were performed on ten chicks from the following age groups: E16–17 (N = 3); E17–19 (N = 3); P0–9 (N = 4).

Cell counts. The density of GABA-I terminals may be a function of NM neuron density. To address this issue, the density of neurons in NM was determined in the nine zones of NM described above by counting cells in 30 μm-thick Nissl-stained sections adjacent to the sections processed for GABA immunocytochemistry. Only cells with a clearly defined nucleus were counted by using the eyepiece reticule method (Konigsmark, '70). Cell density is expressed as the number of cells in a 10,240 μm^2 area.

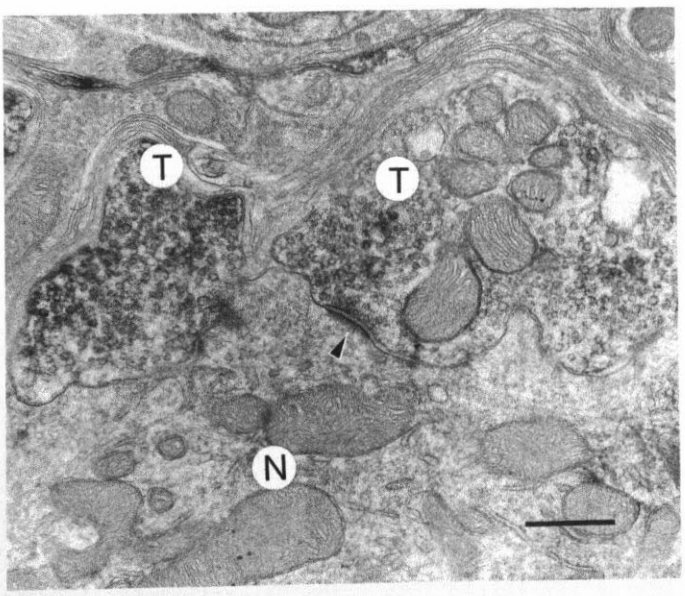

Fig. 3. Two terminals (T) in NM of a posthatch chick (P2) that contain GABA-I. One of these terminals clearly makes a synaptic contact (arrowhead) with a neuronal cell body (N). Scale bar = 500 nm.

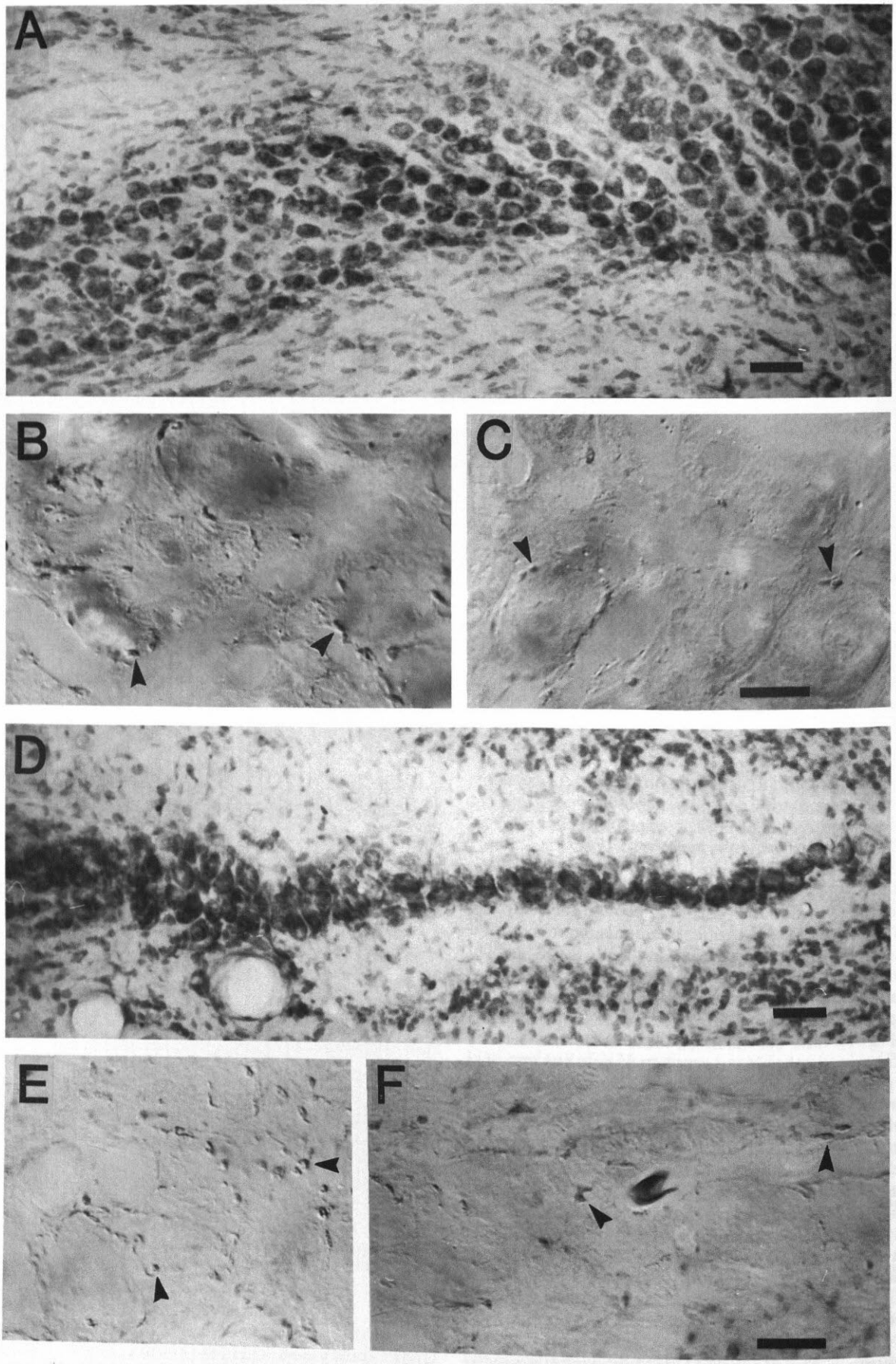

Fig. 4. Nissl-stained sections of NM (**A**) and nucleus laminaris (NL) (**D**) adjacent to those processed for GABA immunocytochemistry (**B, C, E, F**). More GABA-I terminals (arrowheads) appear to be present in lateral (B, E) regions of these nuclei than in medial (C, F) regions. B, C: Nucleus magnocellularis; anti-GABA-BSA 1:4,000. E, F: Nucleus laminaris; anti-GABA-BSA 1:2,000. Dorsal is toward the top and lateral is to the left in each of the photomicrographs. Scale bars = 10 μm (scale bar in C applies to B; scale bar in F applies to E).

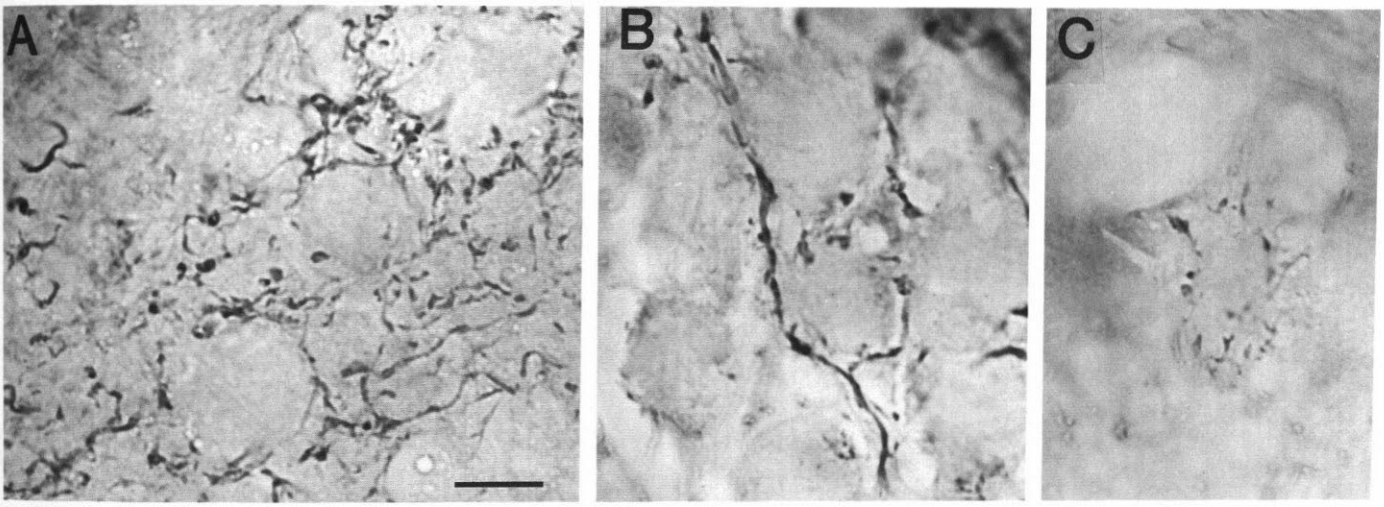

Fig. 5. GABA immunostaining in embryos. **A:** Plexus of varicose fibers in NL; E13; anti-GABA-KLH 1:1,000. Scale bar = 10 μm. **B:** Labeled fibers surrounding an NM cell; E14.5; anti-GABA-BSA 1:4,000. **C:** Preterminal axonal endings around a neuron in NL; E13.5; anti-GABA-BSA 1:4,000. Scale bar in A applies to B and C.

RESULTS

In the present report, the terms GABA-immunoreactive, GABA-positive and GABAergic are used interchangeably to describe all the structures that are immunostained with the GABA-BSA antiserum. The two other antisera described above produced a similar pattern of immunostaining in NM and NL although the GAD-2 immunostaining was more intense than that of the GABA-BSA (compare Fig. 2A and 2C). This is probably due to the fact that the GAD-2 antiserum is a monoclonal antibody raised against chicken (Gottlieb et al., '86). The ABC method provided clearly distinguishable GABA-immunoreactivity against a low background.

Previous investigators using antibodies to GABA or GAD have described small, round, darkly immunostained structures surrounding cell bodies and dendrites at the light microscopic level which are often referred to as "puncta" and thought to represent GABAergic terminals (Müller, '87). We observed similar structures in the chick auditory brainstem which were immunostained with the GABA antiserum and have also confirmed their identity as presynaptic terminals by using EM immunocytochemistry (Fig. 3). Thus, throughout the rest of this paper, we shall refer to these punctate structures as "terminals." Of course, we cannot claim that *all* such structures seen at the light microscopic level are presynaptic terminals.

The qualitative distribution of GABA-I terminals in posthatch chicks will be described first. Then the development of GABA-I in NM and NL will be described in several sections covering embryonic chicks, ages E9–15, E16–17, and E17–19. Results from the analyses of GABA-labeled terminal density and the development of a gradient in terminal density will be presented in a third section. The location of GABAergic neuronal somata is described in a final section.

Posthatch

Most GABA-I in NM of posthatch chicks is localized to terminals circumscribing nerve cell bodies (Fig. 2C), but they can also be found in the neuropil. Few labeled fibers are present at this time. GABAergic terminals are observed in embryos aged E15 and older and in posthatch chicks. More GABA-I terminals are seen in the caudal and lateral regions of NM than in rostral and medial regions (Fig. 4B,C).

In NL, GABA-labeled terminals appear to surround neuronal perikarya and their proximal dendrites. This is especially evident in medial portions of NL. Laterally, GABA-I terminals appear to be no longer restricted to NL's cell body layer but are also found in the ventral and dorsal neuropil. Increasing numbers of terminals are observed in a rostromedial-to-caudolateral direction across NL (Fig. 4E,F). This pattern parallels that found in NM.

Development of GABA-immunoreactivity

Embryonic days 9–15. From E9–11, there is little GABA-I staining in either NM or NL. Because the medial vestibular nucleus and other surrounding structures are heavily stained with the GABA antiserum at these ages, the absence of GABA-I in NM and NL is probably not the result of negative staining due to processing artifact or other variables unrelated to the structure of NM or NL.

At E12–14, a few GABA-I structures are observed in NM and NL. The positively stained structures resemble short and stubby fibers which appear either singly or organized into networks or plexuses (Fig. 5A). Long fibers or axons with varicosities along their length are also discernible. These fibers can be found apposed to cell bodies (Fig. 5B), running horizontally through the neuropil, or passing through NM and NL tangentially. Immunostained structures reminiscent of preterminal axonal swellings are also observed (Fig. 5C). GABAergic terminals are scarce at this time.

Around E15, GABA-I terminals first make their appearance. In NM, many terminals surround nerve cell bodies but some are also located in the neuropil. Labeled fibers appear more numerous and longer than at E12–14. In some tissue sections, there appears to be a transition in the immunostaining pattern of these structures across the mediolateral

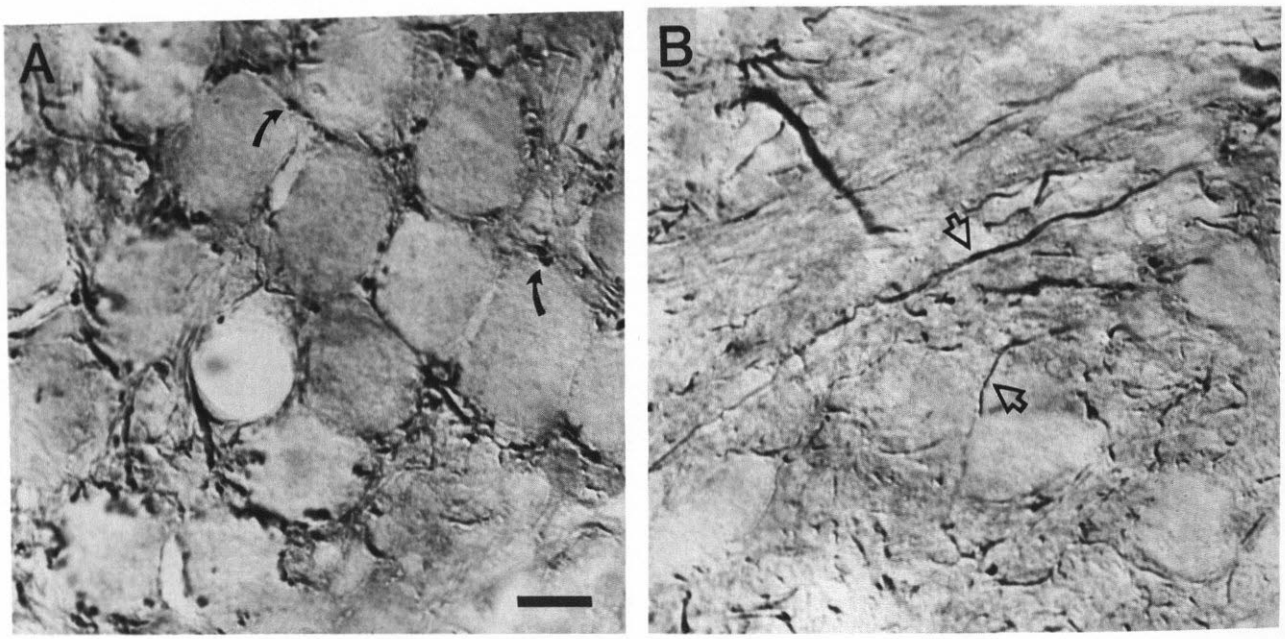

Fig. 6. Transition in the pattern of GABA immunostaining in an E15 embryo; anti-GABA-KLH 1:1,000. **A:** GABA-I terminals (black arrows) in medial NM. **B:** GABA-I fibers (open arrows) in lateral NM from the same section. Scale bar = 10 μm. (scale bar in A applies to B).

extent of NM such that more GABA-I terminals appear to be located medially (Fig. 6A), whereas GABA-labeled fibers appear concentrated in lateral regions of NM (Fig. 6B).

Embryonic days 16–17. Fewer GABA-I fibers and more terminals are observed in NM and NL at E16–17 than at E15. GABAergic terminals are clearly located around nerve cell bodies and in the neuropil of NM and NL. Within NM, GABA-I terminals appear to be uniformly distributed.

Embryonic days 17–19. During the late stages of embryogenesis (E17–19), GABA-labeled fibers are scarce, and the number of GABA-I terminals circumscribing neuronal somata appears to increase. Now, these terminals appear to be denser in caudolateral regions of NM than in rostromedial regions.

Quantitative analysis of the density of GABAergic terminals

Embryonic days 16–17. The density of GABA-I terminals in NM was quantitatively analyzed beginning at the age when the terminals were the predominant structures immunostained—that is, at E16. As noted above, at this age GABAergic terminals appear to be uniformly distributed throughout NM. Quantitative analyses confirmed this observation. Figure 7A shows the density of GABA-I terminals across the mediolateral extent of NM at the caudal, mid-, and rostral levels of the nucleus from one representative chick. There are no significant differences in the density of GABAergic terminals between any mediolateral or any rostrocaudal areas of NM. Data from two other chicks were similarly analyzed, combined, and are depicted in Figure 7B. No spatial gradient in the density of GABA-I terminals is evident in NM at this time.

Embryonic days 17–19. Qualitatively, there appear to be more GABAergic terminals in caudolateral regions of NM than in rostromedial regions. Quantitative analyses support this observation. Figure 7C typifies the distribution of GABA-I terminal density in NM in a single animal, while Figure 7D represents the combined data from three animals. In the lateral area of NM, the density of GABA-I terminals at both the midlevel and the caudal level of the nucleus is greater than that at the rostral level (Fig. 7C). In addition, the density of terminals in the central area of NM at the caudal level is greater than that at the rostral or midlevels. A gradient of increasing density of GABA-I terminals from rostromedial to caudolateral regions of NM is apparent at this age especially at midlevel and caudal levels of the nucleus.

Posthatch. In posthatch chicks (P0–9), quantitative analyses demonstrated a greater density of GABA-labeled terminals in caudolateral regions of NM compared with rostromedial regions. Figure 7E is a graph of the density of GABA-I terminals across the mediolateral extent of NM at the caudal, midlevel, and rostral levels of the nucleus from one posthatch chick. The density of GABAergic terminals in all mediolateral areas of NM at the caudal and midlevels is greater than that in all mediolateral areas of NM at the rostral level. In addition, the density of terminals in the medial and central areas of NM at the caudal level is greater than that in those areas at the midlevel. Overall, the density of GABA-I terminals increases from rostromedial to caudolateral regions of NM. The density of GABA-I terminals in NM was similarly analyzed in three other posthatch chicks. Combined data from these four chicks are summarized in Figure 7F. A spatial gradient in the density of GABAergic terminals which increases in a rostromedial-to-caudolateral direction across NM is evident in the combined data.

The spatial gradient in the density of GABA-immunopositive terminals does not appear to be related to the density of cells in NM. Counts of neurons in rostral, midlevel,

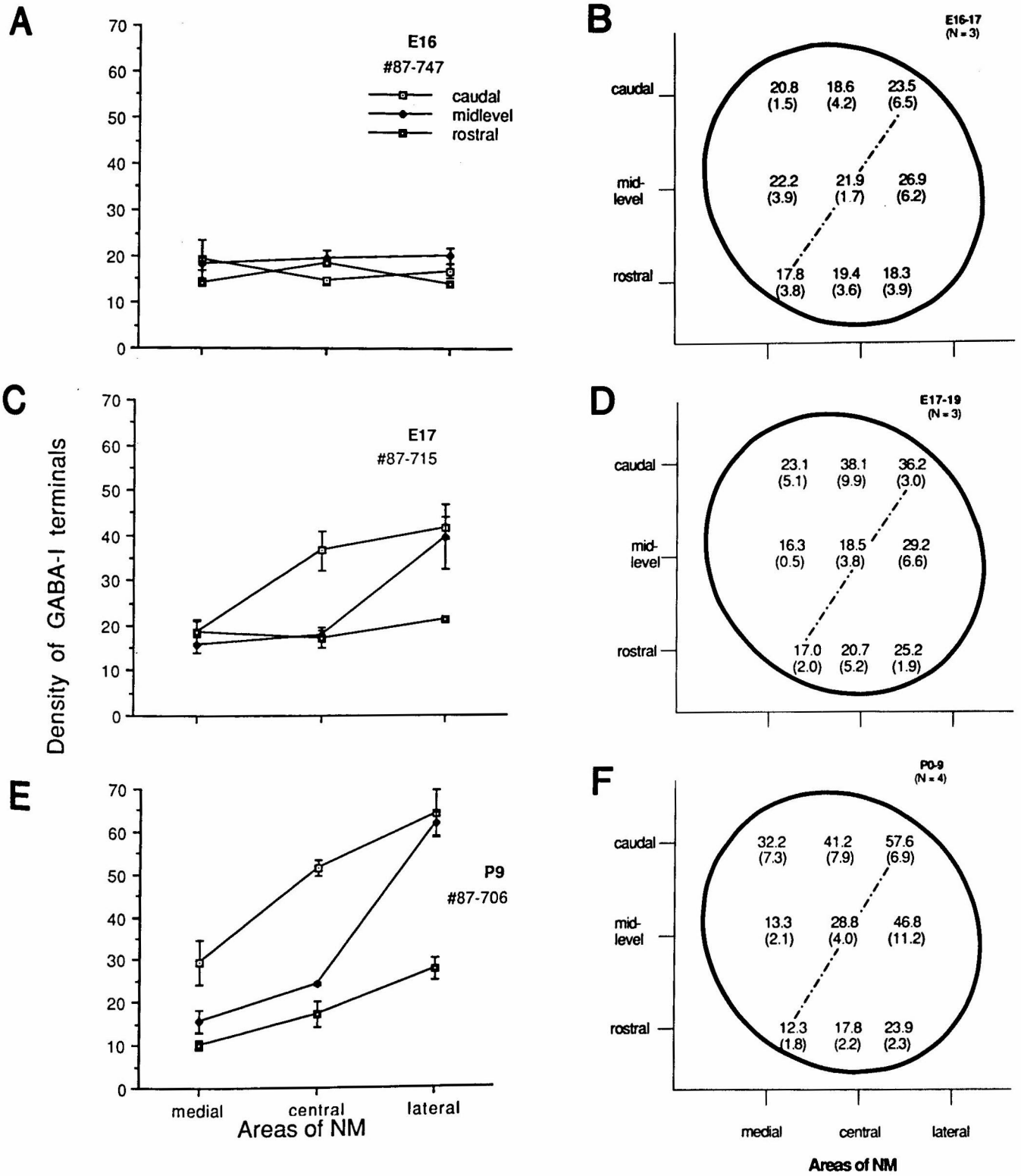

Fig. 7. A,C,E: Terminal density is expressed as the mean number of GABA-I terminals/2,500 μm^2 (±standard error) in nucleus magnocellularis (NM). B,D,F: Means of the density of GABA-I terminals (±standard error of the means) combined from several animals (number in parentheses in upper-right-hand corner) for each of the three age groups. The heavy line represents the approximate boundary of NM as viewed in a horizontal planar projection. The dotted line represents the approximate orientation of the tonotopic axis in NM (high frequencies, rostromedially; low frequencies, caudolaterally). **A:** Data from one E16 chick. The caudal level is 17.9% of the P-A length of NM; the midlevel is 50%; the rostral level is 75.0%. Note the uniform distribution in the density of GABA-I terminals across NM. **B:** Combined data from three chick embryos (E16–17). For each point, the number of sampling areas (N_s) = 9 except for the rostromedial and rostrolateral regions where N_s = 7 due to the small size of the nucleus at this age; the rostrocentral zone where N_s = 8; and the caudolateral zone where N_s = 6 due to the loss of a tissue section. Note that no gradient in the density of GABA-I terminals is evident at this age as compared to chicks aged P0–9 and E17–19. **C:** Data from one E17 chick. The caudal level is 17.9% of the P-A length of NM; the midlevel is 46.4%; the rostral level is 82.0%. Note the appearance of a spatial gradient in the density of GABA-I terminals in a rostromedial-to-caudolateral direction across NM. **D:** Combined data from three embryonic chicks (E17–19). For each point, N_s = 9 except for the rostromedial and rostrolateral regions where N_s = 6. **E:** Data from one posthatch chick, age P9. The caudal level is 21.1% of the posterior-anterior (P-A) length of NM; the midlevel is 47.4%, and the rostral level is 78.9%. Note the increasing density of GABA-I terminals from rostromedial to caudolateral regions of NM. **F:** Data from four posthatch chicks (ages P0–9). For each point, the number of sampling areas (N_s) equals 12, except for the rostromedial and rostrolateral regions where N_s = 9. Note that a rostromedial-to-caudolateral gradient is clearly evident across the nucleus.

TABLE 2. NM Cell Densities for Three Posthatch Chicks (P0–8)

Rostrocaudal levels of NM	Mediolateral areas of NM[1]		
	Medial	Central	Lateral
Rostral	6.8 (1.6)	7.1 (0.8)	8.4 (1.4)
Midlevel	7.0 (0.8)	6.3 (0.7)	6.0 (1.3)
Caudal	7.2 (0.7)	7.5 (0.6)	6.0 (0.8)

[1]Mean number of cells/10,240 μm^2 (standard error).

and caudal regions of NM from three posthatch chicks revealed a uniform distribution in the density of neurons across the nucleus (Table 2).

Development of the gradient

The axis of the spatial gradient of GABA-I terminal density falls roughly on a line drawn from rostromedial to caudolateral in NM. For each of the three age groups, this axis is shown as a dotted line in Figure 7B, D, and F and is plotted in Figure 8. The slope of this function was determined by linear regression analysis. At E16–17, the slope is relatively flat (2.85), while at E17–19, the slope has increased to 9.6. The slope of this axis is steepest for posthatch chicks (22.65). A one-way analysis of variance (ANOVA) using individual slopes from chicks in each of the three age groups revealed a reliable difference [$F(2, 7) = 10.09$, $P < .01$]. A post hoc Newman-Keuls' paired comparison confirmed that the mean slope of the posthatch group was significantly greater than the mean slopes of both the embryonic groups. The slopes of the embryonic groups were not reliably different from each other. Thus, the slope of the gradient in the density of GABA-I terminals in NM increases as a function of the age of the animal.

The data in Figure 8 also suggest that the density of GABA-I terminals in rostromedial zones of NM does not change as a function of age. Rather, it appears that the density increases in caudolateral zones during the later stages of development. An age-by-position analysis of variance (ANOVA) revealed a reliable effect of age [$F(2, 6) = 6.62$, $P < .05$], position [$F(2, 12) = 25.22$, $P < .001$], and an age × position interaction [$F(4, 12) = 4.88$, $P < .05$]. A post hoc Newman-Keuls' paired comparison confirmed that the density of GABA-I terminals in the caudolateral zone of NM in posthatch chicks was greater than the density of terminals in all other areas of NM and greater than in all areas in the other age groups. No other differences were reliable.

Summary

The development of GABA-I in the auditory brainstem nuclei of the chick occurs in several stages. E9–11 is characterized by a virtual absence of immunostaining in NM and NL. Around E12, GABA-I fibers appear. With time, the number and length of these fibers increase. Around E15, GABA-I terminals first make their appearance. The number of labeled fibers progressively decreases while the terminals become organized into a spatial gradient of increasing density along a rostromedial-to-caudolateral axis within NM, characteristic of the pattern in posthatch chicks.

GABA-I cells

GABA-I neuronal somata were observed in the embryonic auditory brainstem beginning about day E11 and in posthatch chicks. They were found most often surrounding both NM and NL and between these two nuclei in the neuropil ventral to NM and dorsal to NL (Fig. 9A). Many GABA-I cells were also found in the neuropil dorsolateral to NL.

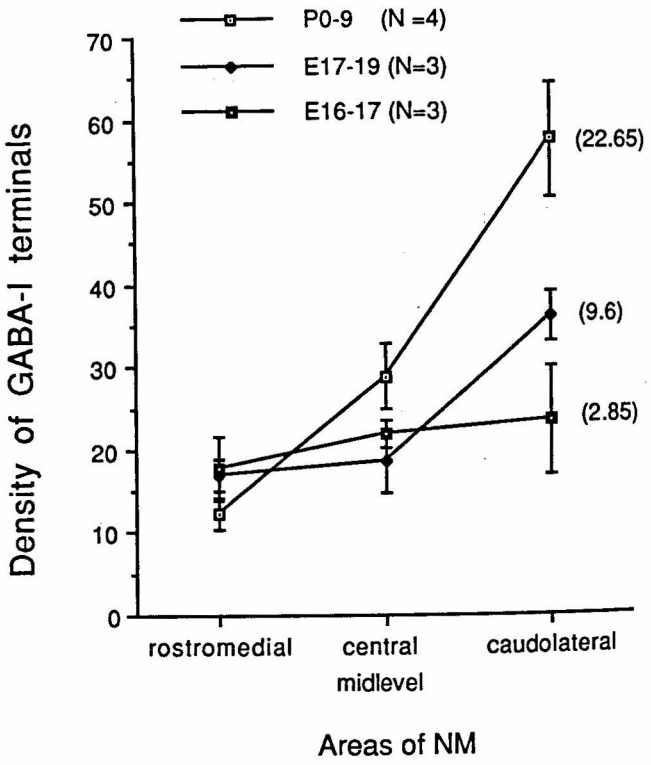

Fig. 8. The development of the spatial gradient of GABA-I terminal density (per 2,500 μm^2) in NM. The axis of the gradient falls roughly on a line drawn through the rostromedial, central midlevel, and caudolateral regions of NM. The slope of this axis was determined for each age group by linear regression analysis and is indicated by the number in parentheses. At E16–17, the slope of the axis of the gradient is relatively flat (2.85), but at E17–19, the slope of the axis has increased to 9.6. The slope of the axis is steepest at P0–9 (22.85). N equals the number of animals that were quantitatively analyzed for each age group. Error bars represent the standard error of the means (SEMs).

In addition, an occasional GABA-I cell was observed among the cell bodies within the borders of NM and NL. These cells were found in embryonic chicks (Fig. 9B) and in posthatch chicks as old as P45 (Fig. 9C) although they were very few in number at both ages. Nucleus angularis (NA), the presumed homologue of the mammalian posteroventral and dorsal cochlear nuclei, contained slightly more GABA-positive cells than either NM or NL. These were found mostly in NA's superficial layers (Fig. 9D).

DISCUSSION

Immunostaining variability within and across species

With the immunocytochemical techniques used here, there is some interanimal variability in the absolute number of GABA-I terminals in a particular zone of NM. This variability may be due to a number of factors: 1) overfixation, which may mask the antigenicity of GABA in the tissue, 2) underfixation, which may cause the antigen of interest to be lost during buffer rinses or incubations, 3) different incubation times in the GABA antiserum, or 4) slight differences in

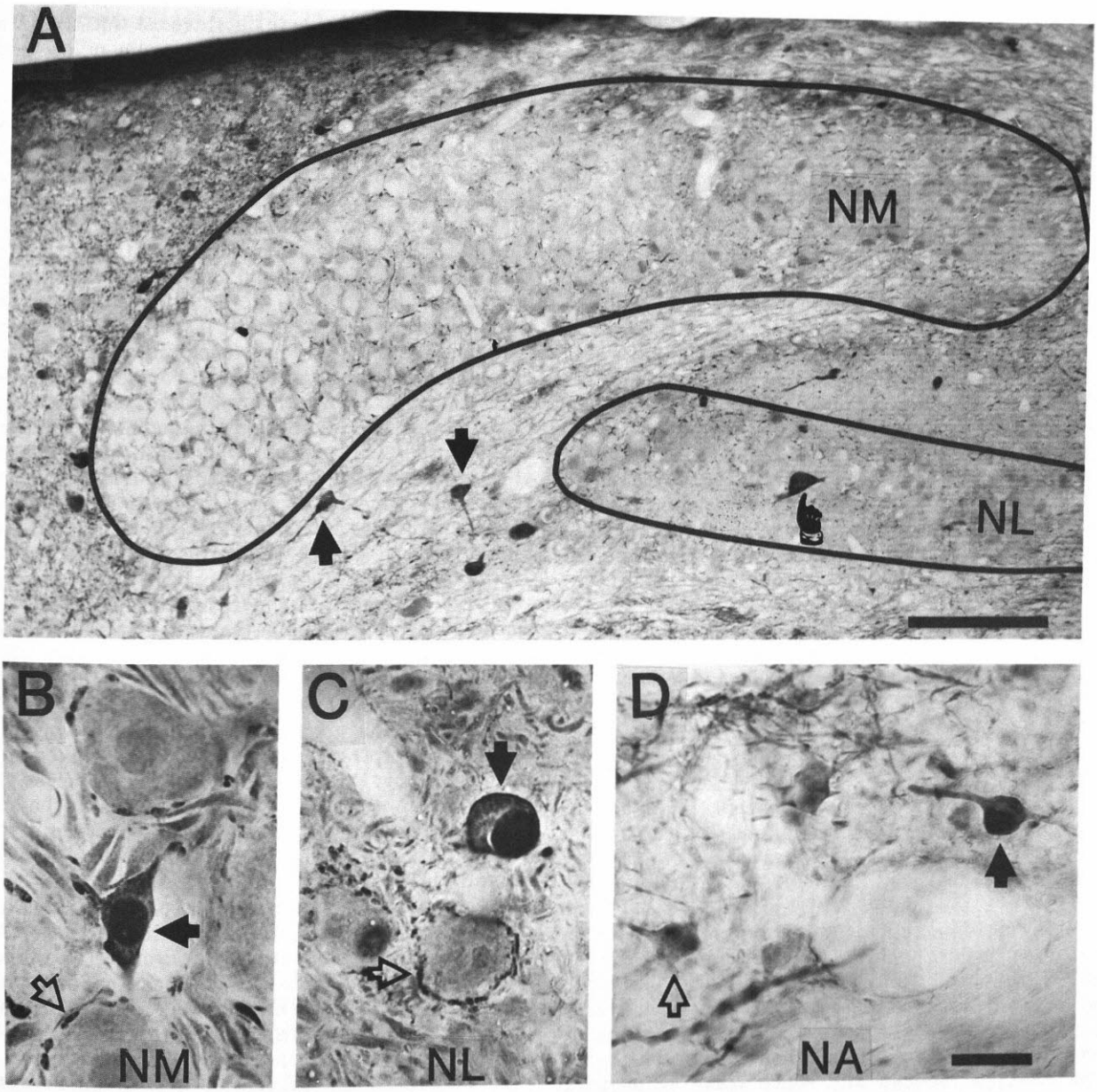

Fig. 9. **A:** GABA-labeled cells surrounding (black arrows) NM and within (pointer NL); E14.5; anti-GABA-BSA 1:4,000. Scale bar = 100 μm. **B:** GABAergic cell (black arrow) in NM. Note GABA-I terminals (open arrow) surrounding adjacent, large, unlabeled NM neurons. P45; anti-GABA-BSA 1:4,000. **C:** Darkly stained GABA-I cell (black arrow) in NL. Note adjacent unlabeled cell with numerous GABA-I terminals (open arrow) surrounding it. E12; anti-GABA-BSA 1:4,000. **D:** Darkly stained (black arrow) and lightly stained (open arrow) GABA-I cells in nucleus angularis; E15; anti-GABA-KLH 1:1,000. Scale bar (applies to panels B–D) = 10 μm.

the time of tissue reaction in DAB, which may account for variations in the intensity of the immunostaining. Keeping this interanimal variability at a minimum was accomplished by standardizing the times for incubations as well as by simultaneously processing multiple brains from age-matched animals.

Comparisons of the number of GABA-I terminals in tissue sections from different animals may also be hampered by small differences in their particular P-A level in NM. For example, if there was a maximum difference of 7%, a tissue section from one chick may be at 50% of the total P-A length of NM, while a similar midlevel section from another animal may be at the 43% level.

Because of these nondevelopmental factors that influence the absolute number of GABA-I terminals, it is important to consider the relative distribution of GABA-I terminals across NM and not their absolute numbers. Despite these sources of variability, our results are still statistically significant between groups and demonstrate that the density of GABAergic terminals increases in caudolateral zones of NM during development.

In our observations on the development of GABA-I within the avian auditory brainstem, it was not our intent to impose arbitrarily defined stages on a developing system. However, the immunostaining patterns observed during the periods E9–11, E12–15, E16–19, and P0–9 appeared qualita-

tively different. Similarly, the emergence of terminals around E15–16 seemed a reasonable starting point for our quantitative analysis. These ontogenetic periods should not be viewed as absolute boundaries, but perhaps as guideposts with which to observe and compare other ongoing developmental processes. Indeed, slight variations in the time course of these events (±1 day) may occur between animals.

It is interesting to compare the morphological changes in GABA-I in the chick auditory brainstem nuclei with those seen in other species. In prenatal rat brain, GABA-I is first seen in distinct fiber systems (Lauder et al., '86). Similarly, in the chick NM and NL, the first observable GABA-I structures are fibers. They become evident around E12. These develop from short, unbranched fibers into structures resembling long axonal processes with varicosities along their length, fibers with preterminal thickenings and branches, and ramifying fiber plexuses (Fig. 5). They become more prominent as the animal matures until about E15, when GABA-I terminals appear. With further development, the GABA-labeled fibers in NM progressively disappear and are replaced with terminals which become spatially organized within NM along a rostromedial-to-caudolateral axis of increasing density. These data suggest that GABA is present in developing neurites and then sequestered in axonal terminals. A similar pattern in the development of GAD-positive innervation is observed in the rat cerebellum (McLaughlin et al., '75) and inferior olive (Gotow and Sotelo, '87).

Electron microscopic immunocytochemistry

Results from the present study indicate that terminals containing GABA-I make synaptic contact with the soma of neurons in NM (Fig. 3). It is not known what percentage of the perikaryal surface in NM is apposed by GABAergic terminals. Parks ('81) estimated that about 18% of the cell surface area in NM is occupied by two types of nonprimary endings distinguished by differences in the profiles of their synaptic vesicles and the type of synaptic contacts made. There is little doubt that at least one of these nonprimary endings is GABAergic. It is likely that the GABAergic terminals correspond to the small, flattened endings which contain pleiomorphic vesicles and which make symmetrical contacts in NM (Parks, '81). However, a few glycinergic terminals are also present in NM (Code et al., '89a; Code and Rubel, '89). A more exhaustive EM-ICC study is needed to elucidate the morphology of the vesicles contained within these GABAergic terminals and to confidently identify the type of synapse that they form on NM neurons.

Development of the GABAergic terminal gradient

At E16, GABAergic terminals are uniformly distributed throughout NM. Their density then increases in caudolateral regions of NM but remains unchanged in rostromedial regions. This differential increase in the density of GABAergic terminals in caudolateral regions creates a spatial gradient of increasing terminal density in a rostromedial-to-caudolateral direction across NM. The orientation of this spatial gradient is the same as the tonotopic axis within the nucleus; in NM, low frequencies are represented in caudolateral regions where the density of GABAergic terminals is greatest and high frequencies are represented in rostromedial areas of NM where the density of GABA-I terminals is the lowest. These data suggest that GABA may be differentially involved with the processing of low- and high-frequency information within NM.

The developmental sequence we have observed in the establishment of GABA-I terminals along a rostromedial-to-caudolateral axis within NM is another example of a series of ontogenetic events occurring in a particular spatiotemporal pattern in the avian auditory system. Normal cell death and growth in the total volume of NM take place along a similar rostromedial-to-caudolateral axis (Rubel et al., '76). The proliferation and retraction of dendrites in NM (Parks and Jackson, '84; Young and Rubel, '86) and the commencement of postsynaptic responses to electrical stimulation of the cochlear nerve (Jackson et al., '82) also follow an anteromedial-to-posterolateral course. In nucleus laminaris, cell death, dendritic growth, and elimination of dendritic processes begin at the rostromedial pole and progress caudolaterally (Rubel et al., '76; Smith, '81). Thus, regions of the cochlear nuclei containing high-frequency representations (rostromedial regions) appear to mature before regions containing low-frequency representations (caudolateral regions) (Rubel and Parks, '75; Rubel et al., '76; Jackson et al., '82). Some evidence from mammals suggests a similar developmental trend (Schweitzer and Cant, '84). Curiously, the basilar papilla matures first near its basal or high-frequency end as well (Retzius, 1884; Rubel, '78; Lippe et al., '86), but these events may not be interdependent (Parks and Jackson, '84).

Our finding of a gradient in the distribution of a putative inhibitory neurotransmitter is not without precedent in the central auditory system. A previous study reported that the highest concentration of glycine receptors in the auditory brainstem of the gerbil is located in the high-frequency regions of the anteroventral cochlear nucleus (AVCN), the lateral superior olive (LSO), and the inferior colliculus (Sanes et al., '87). It is interesting to note that, while the direction of the glycine gradient is directly opposite to that of GABA-I in NM, both gradients develop after the onset of hearing (Sanes and Wooten, '87). Glycine has been immunocytochemically localized in the avian cochlear nucleus, but it does not appear to be distributed in a gradient across NM (Code et al., '89a; Code and Rubel, '89).

In mammals, the density of GABAergic terminals is denser in the AVCN than in the medial superior olive (MSO) (Adams and Mugnaini, '87; Moore and Moore, '87; Roberts and Ribak, '87). However, many glycinergic fibers are found in the MSO (Peyret et al., '87). In the chick, on the other hand, qualitative comparisons from tissue used in the present study suggest that the densities of GABAergic terminals in NM and NL are comparable. However, in contrast to the MSO, glycinergic terminals in NL are sparse (Code et al., '89a; Code and Rubel, '89).

Norepinephrine is another example of a putative inhibitory neurotransmitter in the mammalian cochlear nucleus that displays a nonuniform distribution in the density of its fibers in the rat AVCN (Kromer and Moore, '80). In the AVCN of bats, low-frequency regions have a higher density of catecholaminergic fibers than high-frequency regions (Kossl et al., '88).

It is interesting to compare these gradients to the distribution of excitatory neurotransmitters in the cochlear nucleus. In the cat, rat, and guinea pig cochlear nucleus, the distribution of aspartate appears to mirror that of auditory nerve terminals, while the distribution of glutamate is more uniform (Godfrey et al., '77, '78; Wenthold, '78). Other than

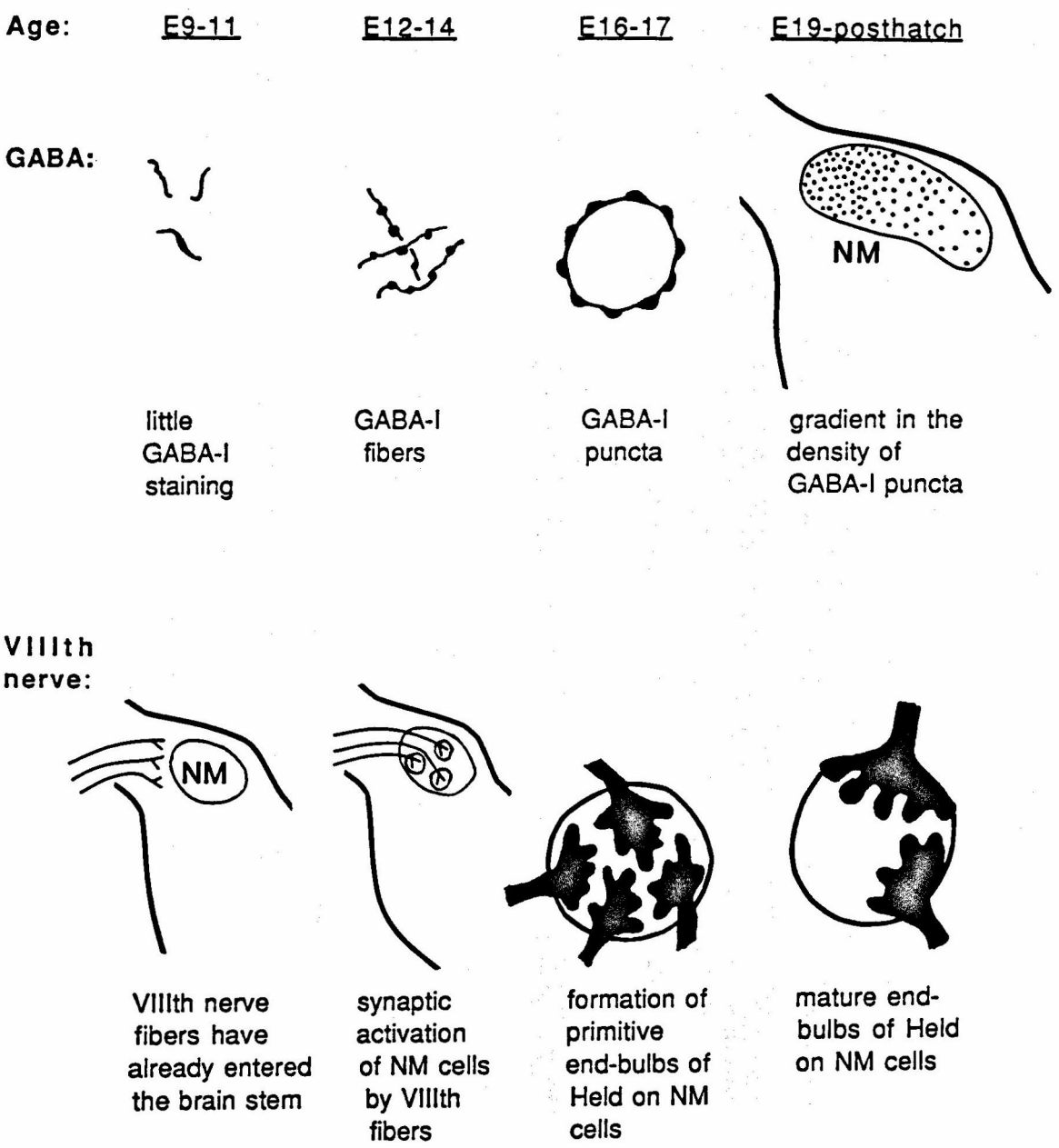

Fig. 10. Temporal sequence in the innervation of NM by GABAergic and auditory nerve inputs.

the present findings on GABA in NM of the chick, the distribution and development of other neurotransmitters in the avian cochlear nucleus have not yet been investigated.

Correlation with VIIIth nerve innervation

The development of GABAergic input to the auditory brainstem appears to be temporally correlated with the development of eighth nerve innervation. Figure 10 summarizes these ontogenetic events. At E9–11, there is little GABA-I within NM. The Golgi method reveals that at this time auditory nerve fibers bear endings in NM resembling growth cones (Jhaveri and Morest, '82b). The first appearance of GABA-I fibers around embryonic day 12 appears to coincide with the development of inner ear function and functional synaptogenesis of VIIIth nerve fibers in NM (Saunders et al., '73; Jackson et al., '82). Around E14, the number of VIIIth nerve axonal branches decreases as they begin to coalesce. Concomitantly, there is a physiologically demonstratable reduction in the number of VIIIth nerve afferents to single NM neurons (Jackson and Parks, '82). GABA-immunostained structures reminiscent of preterminal axonal swellings are observed apposed to cell bodies at this time. By E16, primitive end-bulbs of Held formed by auditory nerve fibers contact NM cells (Jhaveri and Morest, '82b). These investigators also noted a second group of easily distinguishable afferent fibers of unknown origin. This second group of afferents may be the GABAergic terminals which become prominent at this time. By E19, mature end-bulbs of Held are formed on NM cells. GABAergic terminals circumscribing neuronal somata at this time are distributed in a rostromedial-to-caudolateral gradient in NM, characteristic of their posthatch organization.

Possible trophic functions

Evidence that GABA may be involved with increased neurite outgrowth (Wolff et al., '78), regulation of synaptogenesis (Wolff et al., '79; Dames et al., '85), induction of low-affinity GABA receptors (Meier et al., '84), and stimulation of the production of neuron-specific enolase (Meier and Jorgensen, '86) suggests that GABA is involved in neuronotrophic events as well as acting as a neurotransmitter. The temporal coincidence of GABAergic innervation with the morphogenesis of NM cells may be a reflection of GABA's modulatory effects on neuronal development in avian auditory brainstem nuclei.

One intriguing possibility is that the remarkable disappearance of somatic processes on NM cells which begins about E14–15 (Jhaveri and Morest, '82b) and is independent of VIIIth nerve afferents (Parks and Jackson, '84), may be regulated by GABAergic innervation. GABA has been shown to both inhibit and promote neurite elongation of tectal cells grown in serum-free, defined medium (Michler-Stuke and Wolff, '87). It also affects the morphogenesis of pre- and postsynaptic elements in the superior cervical ganglion in vivo (Wolff et al., '87).

GABAergic cells

In the present study, most GABA-immunopositive cell bodies were found surrounding both NM and NL, and within NA, the presumed homologues of the mammalian AVCN, medial superior olive and posteroventral/dorsal cochlear nuclei, respectively. Occasionally, GABAergic cells were also found within NM or within the soma layer of NL. This is in contrast to a previous study which reported no GABA-I cells within either NM or NL in 4–8-week-old chicks (Müller, '87). Since the occurrence of GABA-I neurons within NM and NL is rather infrequent, the absence of GABAergic cells reported in the earlier study may simply be a result of the small sample size of animals used (N = 3). In the present study, based on a much larger number of animals (N = 41), we found a few GABA-positive cells in NM and NL of embryos and in posthatch chicks up to 6 weeks old. Alternatively, the difference may be due to different GABA antisera used in the present study than in Müller's. In addition, it should be recognized that the labeled cells within NM and NL reported here could be glia, which are involved in GABA uptake and degradation, rather than neurons.

The location of GABA-I cells around NL may be related to that of GABAergic cells in the periolivary region of the cat (Adams, '83) and rat (Moore and Moore, '87). In the cat, some cells in the ventral nucleus of the trapezoid body which project to the AVCN are GABAergic (Adams and Wenthold, '87). Thus, the GABAergic cells observed around NL in the chick may be a source of at least some of the GABA-I terminals in NM.

GABAergic neurons have also been reported in the ventral and dorsal cochlear nuclei and in the medial superior olive of the guinea pig (Thompson et al., '85; Peyret et al., '86; Wenthold et al., '86), and in the dorsal cochlear nucleus of the cat (Adams and Mugnaini, '87), rat (Mugnaini, '85; Moore and Moore, '87), and gerbil (Roberts and Ribak, '87). The dorsal cochlear nucleus is known to project to the AVCN in the cat (Lorente de Nó, '33, '76), the mouse (Wickesberg and Oertel, '88), and the horseshoe bat (Feng and Vater, '85). It is possible that GABAergic neurons in nucleus angularis may terminate in NM of the chick. In addition, the GABA-I cells within NM and NL (described above) may be local circuit interneurons that provide some of the GABA-positive terminals observed in both nuclei.

Afferents to NM from the auditory nerve appear not to be the source of GABAergic terminals. After cochlea removal in young posthatch chicks, GABA-labeled terminals remain abundant in the ipsilateral NM (Code et al., '88, '89b). Double-labeling experiments are currently being conducted to determine the origin of the GABAergic input to NM.

NOTE ADDED IN PROOF

We believe that the major source of GABAergic terminals to NM and NL is from local neurons surrounding these two nuclei [von Bartheld, C.S., R.A. Code, and E.W Rubel (1989) GABAergic neurons in brainstem auditory nuclei of the chick: distribution, morphology and connectivity. J. Comp. Neurol., in press.]

ACKNOWLEDGMENTS

GAD-2 antiserum was kindly provided by Dr. David Gottlieb, Washington University, St. Louis, MO. GABA-KLH antiserum was donated by Dr. Timothy Kingan, University of Arizona, Tucson, AZ. We are indebted to Dr. Richard Hyson for his assistance with the statistical analyses. We greatly appreciate the helpful comments provided by Drs. Donald Born, Elizabeth Osterle, and Karen Canady.

This research was supported by NIH postdoctoral grant HD07239 to R.A.C., NIH grant NS24522 to E.WR., and NIH grant NS23701 to G.D.B.

LITERATURE CITED

Adams, J.C. (1983) Cytology of periolivary cells and the organization of their projections in the cat. J. Comp. Neurol. *215*:275–289.

Adams, J.C., and E. Mugnaini (1987) Patterns of glutamate decarboxylase immunostaining in the feline cochlear nuclear complex studied with silver enhancement and electron microscopy. J. Comp. Neurol. *262*:375–401.

Adams, J.C., and R.J. Wenthold (1987) Immunostaining of GABA-ergic and glycinergic inputs to the anteroventral cochlear nucleus. Soc. Neurosci. Abstr. *13*:1259.

Boord, R.L., and G.L. Rasmussen (1963) Projection of the cochlear and lagenar nerves on the cochlear nuclei of the pigeon. J. Comp. Neurol. *120*:463–475.

Born, D.E. (1986) The Role of Neural Activity in Regulating the Structure and Function of Auditory Neurons. Ph.D. dissertation, University of Virginia, Charlottesville, VA.

Born, D.E., and E.W Rubel (1984) Cochlea removal eliminates physiological activity in brain stem auditory nuclei of the chicken. Soc. Neurosci. Abstr. *10*:843.

Cant, N.B. (1981) The fine structure of two types of stellate cells in the anterior division of the anteroventral cochlear nucleus of the cat. Neuroscience *6*:2643–2655.

Canzek, V., and J.C. Reubi (1980) The effect of cochlear nerve lesion on the release of glutamate, aspartate, and GABA from cat cochlear nucleus, *in vitro*. Exp. Brain Res. *38*:437–441.

Code, R.A., G.D. Burd, and E.W Rubel (1987) Development of GABA-immunoreactive terminals in chick brain stem auditory nuclei. Soc. Neurosci. Abstr. *13*:543.

Code, R.A., D. Durham, and E.W. Rubel (1988) Effects of unilateral cochlea removal on GABA-immunoreactive terminals in nucleus magnocellularis of the chicken. Eleventh Midwinter Meeting of the Association for Research in Otolaryngology, Clearwater Beach, FL, Jan. 31–Feb. 4, pp. 43–44.

Code, R.A., D. Durham, and E.W Rubel (1989a) Comparison of glycine-, GABA-, and GAD-immunoreactivities in the auditory brain stem of the chick. Twelfth Midwinter Research Meeting of the Association for Research in Otolaryngology, St. Petersburg Beach, FL, p. 33–34.

Code, R.A., D. Durham, and E.W Rubel (1989b) Effects of cochlea removal on GABAergic terminals in nucleus magnocellularis of the chicken. J. Neurosci. (in preparation).

Code, R.A., and E.W Rubel (1989) Glycine-immunoreactivity in the auditory brain stem of the chick. Hear. Res, in press.

Dames, W., F. Joo, O. Feher, J. Toldi, and J.R. Wolff (1985) γ-Aminobutyric acid enables synaptogenesis in the intact superior ganglion of the adult rat. Neurosci. Lett. *54*:159–164.

Feng, A.S., and M. Vater (1985) Functional organization of the cochlear nucleus of the rufous horseshoe bat (*Rhinolophus rouxi*): Frequencies and internal connections are arranged in slabs. J. Comp. Neurol. *235*:529–553.

Fisher, S.K., and W.E. Davies (1976) GABA and its related enzymes in the lower auditory system of the guinea pig. J. Neurochem. *27*:1145–1155.

Godfrey, D.A., J.A. Carter, S.J. Burger, O.H. Lowry, and F.M. Matchinsky (1977) Quantitative histochemical mapping of candidate transmitter amino acids in cat cochlear nucleus. J. Histochem. Cytochem. *25*:417–431.

Godfrey, D.A., J.A. Carter, O.H. Lowry, and F.M. Matschinsky (1978) Distribution of gamma-aminobutyric acid, glycine, glutamate and aspartate in the cochlear nucleus of the rat. J. Histochem. Cytochem. *26*:118–126.

Gotow, T., and C. Sotelo (1987) Postnatal development of the inferior olivary complex in the rat: IV. Synaptogenesis of GABAergic afferents, analyzed by glutamic acid decarboxylase immunocytochemistry. J. Comp. Neurol. *263*:526–552.

Gottlieb, D.I., Y.-C. Chang, and J.E. Schwob (1986) Monoclonal antibodies to glutamic acid decarboxylase. Proc. Natl. Acad. Sci. USA *83*:8808–8812.

Hackett, J.T., H. Jackson, and E.W. Rubel (1982) Synaptic excitation of the second and third order auditory neurons in the avian brain stem. Neuroscience *7*:1455–1469.

Hamburger, V., and H.L. Hamilton (1951) A series of normal stages in the development of the chick embryo. J. Morphol. *88*:49–92.

Hsu, S.M., L. Raine, and H. Ganger (1981) The use of avidin-biotin-peroxidase complex (ABC) in immunoperoxidase techniques: A comparison between ABC and unlabeled antibody (PAP) procedures. J. Histochem. Cytochem. *29*:577–580.

Jackson, H., J.T. Hackett, and E.W Rubel (1982) Organization and development of brain stem auditory nuclei in the chick: Ontogeny of postsynaptic responses. J. Comp. Neurol. *210*:80–86.

Jackson, H., and T.N. Parks (1982) Functional synapse elimination in the developing avian cochlear nucleus with simultaneous reduction in cochlear nerve axon branching. J. Neurosci. *2*:1736–1743.

Jhaveri, S., and D.K. Morest (1982a) Neuronal architecture in nucleus magnocellularis of the chicken auditory system with observations on nucleus laminaris: A light and electron microscope study. Neuroscience *7*:809–836.

Jhaveri, S., and D.K. Morest (1982b) Sequential alterations of neuronal architecture in nucleus magnocellularis of the developing chicken: A Golgi study. Neuroscience *7*:837–853.

Konigsmark, B.W. (1970) Methods for the counting of neurons. In W.J.H. Nauta and S.O.E. Ebbesson (eds): Contemporary Research Methods in Neuroanatomy. New York: Springer-Verlag, pp. 315–340.

Kossl, M., M. Vater, and H. Schweizer (1988) Distribution of catecholamine fibers in the cochlear nucleus of horseshoe bats and mustache bats. J. Comp. Neurol. *269*:523–534.

Kromer, L.F., and R.Y. Moore (1980) Norepinephrine innervation of the cochlear nuclei by locus coeruleus neurons in the rat. Anat. Embryol. (Berl.) *158*:227–244.

Lauder, J.M., V.K.M. Han, P. Henderson, T. Verdoorn, and A.C. Towle (1986) Prenatal ontogeny of the GABAergic system in the rat brain: An immunocytochemical study. Neuroscience *19*:465–493.

Lippe, W.R., B.M. Ryals, and E.W Rubel (1986) Development of the place principle. In R.N. Aslin (ed): Advances in Neural and Behavioral Development, Vol. 2. Ablex Publishing Corp., pp. 155–203.

Lorente de Nó, R. (1933) Anatomy of the eighth nerve. III.-General plan of structure of the primary cochlear nuclei. Laryngoscope *43*:327–350.

Lorente de Nó, R. (1976) Some unresolved problems concerning the cochlear nerve. Ann. Otol. Rhinol. Laryngol. *85*:[Suppl. 34]:1–28.

McLaughlin, B.J., J.G. Wood, K. Saito, E. Roberts, and J.-Y. Wu (1975) The fine structural localization of glutamate decarboxylase in developing axonal processes and presynaptic terminals of rodent cerebellum. Brain Res. *85*:355–371.

Meier, E., J. Drejer, and A. Schousboe (1984) GABA induces functionally active low-affinity GABA receptors on cultured cerebellar granule cells. J. Neurochem. *43*:1737–1744.

Meier, E., and O.S. Jorgensen (1986) γ-aminobutyric acid affects the developmental expression of neuron-associated proteins in cerebellar granule cell cultures. J. Neurochem. *46*:1256–1262.

Michler-Stuke, A., and J.R. Wolff (1987) Facilitation and inhibition of neurite elongation by GABA in chick tectal neurons. In D.A. Redburn and A. Schousboe (eds): Neurotrophic Activity of GABA During Development. Neurology and Neurobiology, Vol. 32. New York: Alan R. Liss, Inc., pp. 253–266.

Moore, J.K., and R.Y. Moore (1987) Glutamic acid decarboxylase-like immunoreactivity in brainstem auditory nuclei of the rat. J. Comp. Neurol. *260*:157–174.

Mugnaini, E. (1985) GABA neurons in the superficial layers of the rat dorsal cochlear nucleus: Light and electron microscopic immunocytochemistry. J. Comp. Neurol. *235*:61–81.

Müller, C.M. (1987) γ-aminobutyric acid immunoreactivity in brainstem auditory nuclei of the chicken. Neurosci. Lett. *77*:272–276.

Parks, T.N. (1981) Morphology of axosomatic endings in an avian cochlear nucleus: Nucleus magnocellularis of the chicken. J. Comp. Neurol. *203*:425–440.

Parks, T.N., and H. Jackson (1984) A developmental gradient of dendritic loss in the avian cochlear nucleus occurring independently of primary afferents. J. Comp. Neurol. *227*:459–466.

Parks, T.N., and E.W Rubel (1975) Organization and development of brain stem auditory nuclei of the chicken: Organization of projections from N. magnocellularis to N. laminaris. J. Comp. Neurol. *164*:435–448.

Parks, T.N., and E.W Rubel (1978) Organization and development of the brain stem auditory nuclei of the chicken: Primary afferent projections. J. Comp. Neurol. *180*:439–448.

Peyret, D., G. Campistron, M. Geffard, and J.-M. Aran (1987) Glycine immunoreactivity in the brainstem auditory and vestibular nuclei of the guinea pig. Acta Otolaryngol. (Stockh.) *104*:71–76.

Peyret, D., M. Geffard, and J.-M. Aran (1986) GABA immunoreactivity in the primary nuclei of the auditory central nervous system. Hear. Res. *23*:115–121.

Pfeiffer, R.R. (1966) Classification of response patterns of spike discharges for units in the cochlear nucleus: Tone-burst stimulation. Exp. Brain Res. *1*:220–235.

Ramón y Cajal, S. (1908) Les ganglions termineaux du nerf acoustique des oiseaux. Trav. La. Rech. Biol. (Madrid) *6*:195–224.

Retzius, G. (1884) Das Gehorogan der Wirbeltiere. II: Das Gehorogan der Reptilien, der Vogel und Saugetiere. Stockholm: Samson and Wallin.

Roberts, R.C., and C.E. Ribak (1987) GABAergic neurons and axon terminals in the brainstem auditory nuclei of the gerbil. J. Comp. Neurol. *258*:267–280.

Rubel, E.W (1978) Ontogeny of structure and function in the vertebrate auditory system. In M. Jacobson (ed): Handbook of Sensory Physiology, Vol. IX. New York: Springer-Verlag, pp. 135–237.

Rubel, E.W, and T.N. Parks (1975) Organization and development of brain stem auditory nuclei of the chicken: Tonotopic organization of n. magnocellularis and n. laminaris. J. Comp. Neurol. *164*:411–434.

Rubel, E.W., D.J. Smith, and L.C. Miller (1976) Organization and development of brain stem auditory nuclei of the chicken: Ontogeny of n. magnocellularis and n. laminaris. J. Comp. Neurol. *166*:469–490.

Sanes, D.H., W.A. Geary, G.F. Wooten, and E.W Rubel (1987) Quantitative distribution of the glycine receptor in the auditory brain stem of the gerbil. J. Neurosci. *7*:3793–3802.

Sanes, D.H., and G.F. Wooten (1987) Development of glycine receptor distribution in the lateral superior olive of the gerbil. J. Neurosci. *7*:3803–3811.

Saunders, J.C., R.B. Coles, and G.R. Gates (1973) The development of auditory evoked responses in the cochlea and cochlear nuclei of the chick. Brain Res. *63*:59–74.

Schweitzer, L., and N.B. Cant (1984) Development of the cochlear innervation of the dorsal cochlear nucleus of the hamster. J. Comp. Neurol. *225*:228–243.

Smith, Z.D.J. (1981) Organization and development of brain stem auditory nuclei of the chicken: Dendritic development in n. laminaris. J. Comp. Neurol. *203*:309–333.

Smith, D.J., and E.W Rubel (1979) Organization and development of brain stem auditory nuclei of the chicken: Dendritic gradients in nucleus laminaris. J. Comp. Neurol. *186*:213–240.

Thompson, G.C., A.N. Cortez, and D.M.-K. Lam (1985) Localization of GABA immunoreactivity in the auditory brainstem of guinea pigs. Brain Res. *339*:119–122.

Wenthold, R.J. (1978) Glutamic acid and aspartic acid in subdivisions of the

cochlear nucleus after auditory nerve lesion. Brain Res. *143*:544–548.

Wenthold, R.J. (1979) Release of endogenous glutamic acid, aspartic acid and GABA from cochlear nucleus slices. Brain Res. *162*:338–343.

Wenthold, R.J., and M.R. Martin (1984) Neurotransmitters of the auditory nerve and central auditory system. In C. Berlin (ed): Recent Advances in Speech, Hearing and Language: Hearing Sciences. San Diego: College-Hill Press, Inc.

Wenthold, R.J., J.M. Zempel, M.H. Parakkal, K.A. Reeks, and R.A. Altschuler (1986) Immunocytochemical localization of GABA in cochlear nucleus of the guinea pig. Brain Res. *380*:7–18.

Wickesberg, R.E., and D. Oertel (1988) Tonotopic projection from the dorsal to the anteroventral cochlear nucleus of mice. J. Comp. Neurol. *268*:389–399.

Wolff, J.R., F. Joo, and W. Dames (1978) Plasticity in dendrites shown by continuous GABA administration in superior cervical ganglion of adult rat. Nature *274*:72–74.

Wolff, J.R., F. Joo, W. Dames, and O. Feher (1979) Induction and maintenance of free postsynaptic membrane thickenings in the adult superior cervical ganglion. J. Neurocytol. *8*:549–563.

Wolff, J.R., F. Joo, and P. Kasa (1987) Synaptic, metabolic and morphogenetic effects of GABA in the superior cervical ganglion of rats. In D.A. Redburn and A. Schousboe (eds): Neurotrophic Activity of GABA During Development. Neurology and Neurobiology, Vol. 32. New York: Alan R. Liss, Inc., pp. 221–252.

Young, S.R., and E.W Rubel (1983) Frequency-specific projections of individual neurons in chick brainstem auditory nuclei. J. Neurosci. *3*:1373–1378.

Young, S.R., and E.W Rubel (1986) Embryogenesis of arborization pattern and topography of individual axons in N. laminaris of the chicken brain stem. J. Comp. Neurol. *254*:425–459.